10-17-1996

Charge-coupled devices with fast timing for astrophysics and space physics research

M L. Cherry
Louisiana State University - Baton Rouge

P P. Altice
Louisiana State University - Baton Rouge

S B. Ellison
Louisiana State University

T G. Guzik
Louisiana State University - Baton Rouge

John R. Macri
University of New Hampshire - Main Campus, John.Macri@unh.edu

See next page for additional authors

Charge-coupled devices with fast timing for astrophysics and space physics research

M. L. Cherry[1], P. P. Altice[1], Jr., S. B. Ellison[1], T. G. Guzik[1], J. R. Macri[2], M. L. McConnell[2], G. Y. McLean[3], J. Ryan[2], P. Suni[3]

[1]Department of Physics & Astronomy, Louisiana State University, Baton Rouge, LA 70803
[2]Space Science Center, University of New Hampshire, Durham, NH 03824
[3]Suni Imaging Microsystems, Inc., Mountain View, CA 94041

ABSTRACT

A charge coupled device is under development with fast timing capability (15 millisecond full frame readout, 30 microsecond resolution for measuring the time of individual pixel hits). The Fast Timing CCD will be used in conjunction with a CsI microfiber array or segmented scintillator matrix detector to detect X-rays and gamma rays with submillimeter position resolution. The initial application will be in conjunction with a coded aperture hard X-ray/gamma ray astronomy instrument. We describe the concept and the readout architecture of the device.

Key Words: Hard X-ray, gamma ray, charge coupled devices, time resolution, coded aperture

1. INTRODUCTION

Charge coupled devices (CCDs) are, in many ways, ideal light detectors. They are high resolution, reliable analog sampled devices with good quantum efficiency over a wide range of wavelengths from the infrared to the X-ray regime. Typically, however, scanning is limited to video rates (30 frames/second). For applications requiring fast timing or dynamic image capture (e.g., high-speed automated inspection on manufacturing or packaging lines, short-duration exposures of rapidly moving objects, surveillance from a moving vehicle or aircraft, or high-resolution microscope studies of transient phenomena under conditions where a mechanical shutter would induce unacceptable vibrations), presently available CCDs may be too slow. A fast timing CCD would have numerous applications for viewing images when either the subject or the camera is in motion. For spectroscopic applications (in non-destructive testing, medical imaging, fluorescence studies, astronomy, material science and surface physics measurements) where no more than a single photon/pixel must be detected in each readout in order to measure the photon energy, a CCD with fast timing capable of isolating individual photons would be extremely useful. In long-duration exposures of low intensity or low contrast objects (for example, radiological searches for small lesions in the presence of motion induced by the patient's breathing, or extended satellite observations of faint astronomical objects in the presence of an ionizing cosmic ray background passing through the detector), a fast timing CCD would allow the final image to be summed from discrete, short-duration individual exposures in which the blurring due to motion can be removed and cosmic ray events can be vetoed. We are currently developing a CCD readout device with 10-30 μsec timing resolution suitable for such applications.

In astronomy, observation of transient or highly variable sources like X-ray binaries or AM Her stars requires time resolution usually available only with photomultiplier tubes. Occultations require millisecond timing, and wide-angle searches for optical counterparts of gamma ray bursts would benefit from good timing resolution as well. Although photomultipliers have nanosecond timing capability, they are not capable of simultaneous wide-field imaging. In addition, photomultipliers are rapidly becoming less and less available at large telescope facilities as they are being replaced by CCDs. The case of hard X-ray/γ-ray astronomy (20-600 keV) offers an interesting example, as described in Sec. 2. The best angular resolution so far available at these energies has been the 13' of arc obtained by the SIGMA satellite experiment[1]. Our group is currently developing the Minute of Arc Resolution Gamma ray Imaging Experiment (MARGIE), a coded aperture instrument designed for a wide field of view and minute of arc resolution[2,3]. MARGIE employs a room-temperature cadmium zinc telluride (CZT) readout[4,5] for the energy range 20-200 keV. At higher energies (50-600 keV) an array of CsI (Tl) microfibers[2,6] or a segmented CsI matrix detector[7] serves as the active X-ray detector, with the optical scintillation from the CsI being detected with a crystal silicon CCD array. Millisecond time resolution is desirable for observing pulsars (e.g., the

Crab) and gamma ray bursts; time resolution ~30 μsec makes it possible to operate in anticoincidence with an active charged particle shield to veto cosmic ray events striking a representative balloon or spacecraft payload once every ≤ 200 μsec. The capability to isolate individual X-ray photons is required to measure photon energies.

In order to satisfy the requirements for a coded aperture X-ray/γ-ray imager with 1' resolution, a Bi-Directional Fast Timing CCD is being developed for use with existing CsI microfiber arrays or segmented CsI matrix detectors. The CCD development involves two main efforts: 1) The inter-pixel charge transfer requires a new on-chip clocking architecture. 2) The readout will require a low-noise multi-input amplifier-sample/hold-multiplexor incorporated into a custom CMOS Application Specific Integrated Circuit (ASIC) mated to the CCD. Position-sensitive CsI microfiber arrays and the capabilities of currently available CCDs, with particular reference to the X-ray/γ-ray astronomy application, are discussed in Sec. 3. The concept of the Bi-Directional Fast Timing CCD and the CCD/ASIC development are described in Sec. 4.

2. POTENTIAL APPLICATIONS

2.1. X-ray/γ-Ray Astrophysics and Solar Physics

Angular resolution is an essential ingredient in hard X-ray and γ-ray observations of solar flares and discrete astrophysical sources. Improvements in angular resolution permit the identification of individual sources, both isolated sources and those located in crowded regions of the sky; reduce the number of candidate sources in detector error boxes on the sky; and improve the signal-to-noise for discrete sources. The development described here will be applicable to either a satellite or balloon-borne coded aperture hard X-ray telescope designed to cover the energy range 20 - 600 keV with a wide field of view (6-30° half angle) and angular resolution 2-6'.

In the coded aperture approach, a uniformly redundant array (URA) mask pattern minimizes the sidelobes in the reconstructed image of the sky by requiring that the autocorrelation gives a delta function spike in the direction of a source, and gives a uniform background in other directions. A further advantage of the coded aperture approach is that source and background are measured simultaneously, thereby minimizing systematic effects caused by time- or zenith angle-dependent background changes. Other coded aperture instruments have worked successfully at both lower and higher energies: SIGMA[1] covered the energy range up to 1.3 MeV, with 13' angular resolution; GRIP[8] worked up to 5 MeV with 0.6° resolution; DGT[9] observed up to 9.3 MeV with 3.8° angular resolution; and ART-P[10] operated over the range 4-60 keV with 6' resolution. We have chosen to optimize our efforts for the energy range 20-600 keV.

A high angular resolution, broad field-of-view hard X-ray instrument would be able to address many outstanding scientific questions in astrophysics and solar physics. Possible scientific goals which could be addressed include:

- Search for positron line emission both at 511 keV and (redshifted) at lower energies from pulsars, gamma ray bursts, black hole candidates, the Galactic Center, and (utilizing the wide field of view) the Galactic Plane;
- provide measurements of the spectrum and source position of γ-ray bursts in the 20-600 keV range with both a wide field of view and minute of arc angular resolution. By correlating such observations at several wavelengths our understanding of this most baffling class of high energy sources would be greatly facilitated;
- provide high sensitivity spectral studies in the 20-600 keV region to distinguish between high-temperature thermal sources and low-temperature sources with hard non-thermal tails;
- provide extensive sky coverage at high angular resolution;
- search for additional gamma-ray pulsars;
- study the accretion flows and neutron star magnetopheres of X-ray binaries in the 20-600 keV energy band where little is known about the detailed emission processes;
- provide spectral shape measurements and temporal studies of Cygnus X-1 and other candidate galactic black hole binary systems to determine the electron temperature at the source, study the "high-energy tail" emission and evaluate models of the γ-ray emission;
- provide high angular resolution AGN measurements to correlate with higher energy CGRO observations and study the contribution of AGNs to the diffuse cosmic background;
- observe crowded source regions such as the Galactic Center providing spectral measurements with high angular resolution over an extended, contiguous time period (10-20 days for a long duration balloon mission);

- measure the fundamental and higher harmonics of cyclotron features associated with X-ray pulsars to provide an accurate physical interpretation;
- study the morphology of solar flare regions following the population of accelerated electrons and observing the frequency and extent to which these electrons escape the flaring region;
- use the flux of hard X-rays from electron bremsstrahung at several hundred keV as a surrogate for imaging nuclear emissions during solar flares;
- provide new studies of low intensity and high variability emission, either in small flares or brightenings or prior to the hard X-ray and γ-ray emission in larger flares; and
- provide high time and angular resolution of hard X-ray emission over the full solar disk.

CZT provides good sensitivity with ~200 μm position resolution and ≤10 keV (FWHM) energy resolution[4,5]. The 1.5 mm CZT thickness limits us, however, to a maximum energy ~200 keV. Thicker CZT detectors could be used in order to go to higher energies, but then the CZT cost would increase. Rather than use CZT at the high energies, high resolution segmented CsI scintillators have been developed which will provide both the sensitivity and position resolution required.[2,6,7] Fig. 1 shows a photograph of a CsI microfiber array grown at Radiation Monitoring Devices.[2,6] Similar microfiber arrays have been grown with up to 2" diameter, 300 μm thickness, and 125 μm position resolution.

The scintillator readout is accomplished with a CCD array. The CsI (Tl) output spectrum peaks near the same wavelength as the sensitivity of silicon semiconductor detectors (540 nm). The scintillator light yield (20 optical photons/keV) and CCD noise levels (10-25 pA/cm^2 at 20°C thermal, 10 e$^-$/pixel readout noise) combine to give a threshold below 30 keV. Both the CsI and the CCD resolution are better than the coded aperture mask element diameter (0.5 mm), leading to an angular resolution (at 1.5 m mask-detector separation) of 1'. The CCD capabilities are driven largely by the requirements that the detector must be able to measure individual photon energies, and that the detector must operate in the presence of a flux of cosmic ray protons. An anticoincidence shield surrounding the instrument will register a cosmic ray hit every 100-200 μsec, so that a CCD operated in conjunction with this cosmic ray veto must have a time resolution significantly better than 100 μsec. A similar time resolution is appropriate for studies of fast pulsars or for high time resolution studies of gamma ray bursts.

2.2. Medical Imaging

Current X-ray mammography devices typically rely on photographic film. Although film provides significantly better spatial resolution than existing commercially available CCD instruments (which provide resolution of 8-9 line pairs/mm at best), its limited dynamic range and contrast are disadvantages[11,12]. These disadvantages provide real limitations in cases where the radiologist needs to study soft tissue masses or microcalifications in breast tissue, or search for faint lesions in the presence of nearby high-density glandular material, or perform dual-energy comparisons of attenuation in carcinoma and normal tissue[13]. By combining a relatively thick CsI microfiber array with a high resolution Fast-Timing CCD readout, by removing the standard reducing fiber optic taper, and by reducing the noise level (and hence the need for cooling), one has the advantages of potentially lower X-ray exposure for the patient, higher contrast and energy resolution, reduced complexity and cost, and position resolution suitable for detailed diagnostic applications.

As an example, in a mammography examination, a patient's typical X-ray exposure may be on the order of 10^5 X-ray/mm^2. A frequent complaint by physicians is the lack of contrast sometimes seen in dense tissue regions. A solution to this problem is to use higher energy X-rays. As the energy increases, however, the fraction of Compton-scattered photons increases. These show up as photons coming from spurious directions. In other words, Compton scattering produces an unwanted background. In the approximation that tissue is essentially water, then as an example at 60 keV the ratio of the incoherent scattering cross section to the photoelectric cross section is nearly 30 and the situation is severely background-limited. This background can be removed by measuring the individual X-ray energies, which can only be accomplished in a detector with sufficient time resolution to identify individual events.

For a sharp image, one desires a signal-to-noise ratio $\frac{S}{\sqrt{N}}$ ~10 in a single pixel, corresponding to 100 events/pixel in the absence of background (e.g., if the noise can be removed by accepting only events with energy in the photopeak). Let r be the ratio of scattered flux to unscattered flux (where r may be significantly greater than unity). If the energy is not measured and the scattered photons cannot be separated from the unscattered, then $N \sim rS$ and $\frac{S}{\sqrt{rS}} \sim 10$, so that the required number of "good" (unscattered photopeak) events becomes $S \sim 100\ r$. The total number of incident X-rays must then be 100 r^2 per pixel. If a CCD consists of N_{rows} rows x N_{rows} columns with square pixels of pitch d, and each row is read out in a time t_{row} then the total readout time for a frame is $T = N_{rows} \times t_{row}$. If the incident X-rays are detected in some number of frames n, then the required flux is

$$F_{noise} = \frac{100r^2}{d^2 nT} \frac{X-rays}{mm^2-sec}. \tag{1}$$

If, however, the energy can be measured, then only unscattered photopeak X-rays are accepted and N= S = 100. The total number of incident photons is then 100 r and *the patient's dosage is a factor of r lower* than in the previous case:

$$F_{no\ noise} = \frac{100r}{d^2 nT} \frac{x-rays}{mm^2-sec}. \tag{2}$$

For the Fast Timing CCD to measure individual X-ray photons, the flux must be kept sufficiently low that individual events can be resolved. Individual events can be identified if the flux F is sufficiently low that there is no more than 1 event for every 2 columns over the frame readout time T (see Sec. 4.) :

$$F < \frac{1}{2\ N_{rows}\ d^2\ T} = \left(\frac{256}{N_{rows}}\right)^2 \left(\frac{50\mu m}{d}\right)^2 \left(\frac{10\mu sec}{t_{row}}\right) \frac{300}{mm^2\text{-sec}} . \tag{3}$$

In that case, the total exposure time needed to collect 100 events/pixel is

$$t_{exp} = \left(\frac{N_{rows}}{256}\right)^2 \left(\frac{t_{row}}{10\ \mu sec}\right) 130 \text{ sec.} \tag{4}$$

A time of 130 seconds is far too long for a patient to remain stationary, but the observation can readily be broken into small intervals. By the use of fiducial markers on the patient, the images from these small intervals can then be oriented and added together to give a composite image with a potentially significant decrease in total patient X-ray dosage.

3. X-RAY/γ-RAY DETECTOR DEVELOPMENT

3.1 CsI Microfiber Arrays

Although CsI has a reasonably high X-ray absorption cross section, 92% of 300 keV X-rays pass through 1 mm of CsI without interaction (96% at 500 keV). For a 5 mm thickness these fractions of unattenuated photons go down to 65% at 300 keV and 80% at 500 keV. In a uniform, homogeneous scintillator, however, as the detector thickness goes up, the spot size of the emitted scintillation light increases correspondingly: Since the light is emitted essentially isotropically, the spot size diameter is comparable to the detector thickness. One therefore has competing requirements: A thick detector is needed for high detection efficiency, while a thin detector is needed for good position resolution. The X-ray astronomy experiment position resolution requirements demand a spot size <0.5 mm.

CsI microfiber detectors offer a possible solution[2,6]. CsI (Tl) layers are evaporated in such a way that a film is formed of 10 - 100 μm diameter fibers extending from the top to the bottom surface of the film. The elongated fiber structure acts as an array of light pipes to channel light to the bottom surface by total internal reflection. Fig. 1 shows an SEM micrograph of the resulting very regular column structure for a 100μm thick CsI array grown on a fiber optic substrate. Fig. 2 shows a closeup of a 300μm film, and Fig. 3 shows (for comparison) a sample of Gd_2O_2S. Figs. 2 and 3 also show the very regular pattern etched into the fiber optic substrate.

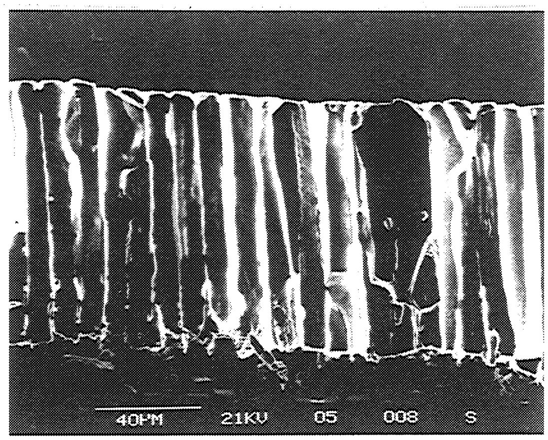

Figure 1. Scanning electron microscope picture of a 100μm thick CsI(Tl) fiber layer deposited at RMD.

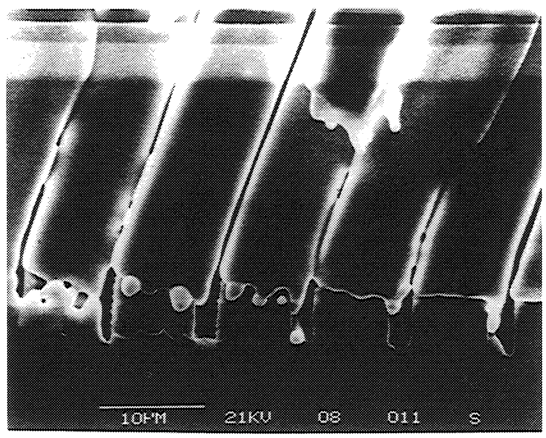

Figure 2. SEM closeup view of 300μm film. The substrate pattern can be seen clearly at the bottom of the columns, with the well-separated CsI fibers growing up from the tops of the substrate pedestals.

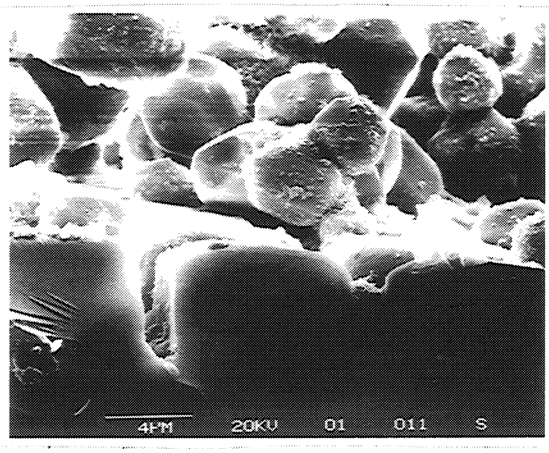

Figure 3. A view shown for comparison of standard granular commercial Gd_2O_2S deposited on the same fiberoptic substrate. The irregular structure and poor packing fraction of standard phosphor screen material compared to our CsI films can be clearly seen.

Light output from 300μm thick CsI arrays is 7 times that of therbium-doped glass scintillators at 70-420 kVp and 1.5 times that of a commercial Lanex screen at 28 kVp. At 200 kVp, the modulation seen with a 14 lp/mm phantom (corresponding to 36μm line separation) is 15%, and 63% at 4 lp/mm (125μm line separation); at 420 kVp, the observed modulation is 20% at 14 lp/mm.

3.2 Standard Optical Readout—Limitations of Currently Available Large Area Silicon Pixel Arrays

The CsI light output can be detected by a CCD array. Perhaps the most suitable commercially available CCD readout is produced by Loral Fairchild. Loral Fairchild currently manufactures CCD full frame image sensor arrays with 15μm pitch in matrices of up to 4096 horizontal by 4096 vertical photosites, corresponding to an area of 62 x 62 mm^2. An array of 6 x 6 such CCD's covers a total area in excess of 1380 cm^2. The structure is composed of individual CCD elements with no empty spaces, so that a fill factor of 85 - 90% is achieved. The readout architecture allows both horizontal and vertical binning, which can speed up the readout time and at the same time permit averaging over blemished pixels (thereby minimizing the need for selecting zero-defect arrays and therefore reducing costs). A further increase in readout speed is achieved by reading out the imaging area into independent 2048 x 4096 upper and lower halves with either separate or common clocking. Video information from each half is provided as a single sequential readout stream of 2048 lines each containing 4096 analogue pulse heights. Quantum efficiency over the range 450-750 nm is ~35%. Dark current is reduced by adding an additional implant under one vertical phase to collect the photoelectrons with all vertical clocks low during the integration interval. At room temperature, this Multi-Pinned Phase operating mode reduces the dark current to 0.025 nA/cm^2 with a further decrease by a factor of 2 for every 4-6°C drop in temperature. Given the observed CsI (Tl) output light level of 20 photons/keV and a 35% CCD quantum efficiency, we expect 350 electron-hole pairs at 50 keV. If the pixels are binned into 8 x 8 "superpixels" (each 120 x 120 μ^2), the full array can be read out in 50 msec (corresponding to 5.2 MHz, as compared to the maximum possible readout rate for the array of 8 MHz). In 50 msec, assuming a moderate cooling of the array from 25°C to a nominal operating temperature of 0°C, the superpixel dark current corresponds to a noise threshold of 8 keV.

For the γ-ray astronomy application, the combination of the Loral Fairchild architecture (which allows both horizontal and vertical binning) and the low photon intensities (compared to medical and dental X-ray beams) permits one to clock the array sufficiently quickly so that a 50 msec frame contains only a small number of pixels above the dark current level. In principle, one could therefore clock 2048 lines out as a single sequential data stream, suppress pixels below a preset threshold (dark current) and above a preset maximum (charged protons) and send the resulting stream of pulse heights to an analog-to-digital converter (ADC), with two ADC's per CCD. A layer of 6 x 6 CCD's could be serviced by a system of 72 ADC channels with a 380 nsec conversion time/channel and a single CPU.

With a readout time of 50 msec, the integration time must be $t_{int} \gtrsim$ 100 msec. For fast timing observations of pulsars and gamma ray bursts, however, it would be desirable to have significantly faster timing. Charged protons passing through the CsI/CCD will be recognized by their large pulse heights; protons striking the mask or shields and generating bremsstrahlung photons will not be easily removed from the data, however, without a capability to measure the event time to better than 100 μsec (the average time between protons striking anywhere on the instrument). The noise, power, and cost constraints imposed by the 5 MHz clocking and 380 nsec ADC conversion time are also significant. In Sec. 4 below, we describe the capabilities of the Bi-Directional Fast Timing CCD being developed at Suni Imaging Microsystems, Inc. to address these issues.

4. BI-DIRECTIONAL FAST TIMING CCD

4.1 CCD Bi-Directional Architecture

With a standard readout architecture, the photosites collect light for some integration time t_{int} >> 50 msec. If a photon strikes a photosite (i,j) during the integration, a photoelectron is generated at that pixel. At the end of the integration, the charge on each pixel is clocked vertically upward one row at a time. After each vertical transfer, one row of charge has been transferred into the horizontal readout register at the top of the chip. Now the individual pixel (column) charge packets in the horizontal readout register can be clocked horizontally to the output amplifier; the entire array is again shifted vertically; the next row is shifted horizontally; and the charge transfer continues until all rows and columns have been shifted to the output amplifier.

Rather than the photon arriving at pixel (i,j) during the integration time, however, imagine that the photon arrives at (i,j) at a time t_γ *after* the start of the readout. If the time between vertical transfers is t_{row}, then t_γ / t_{row} rows will have been clocked upwards by the time the photon arrives at (i,j). A photoelectron will still be produced at (i,j), but it will be read out *as if* it had been produced during the integration time at pixel $(i + t_\gamma / t_{row}, j)$. In the standard situation, a photon arriving during the readout and producing a spurious signal would be considered a background. A shutter is frequently used to block off the CCD during the readout in order to prevent this background.

In the case of low fluxes, however, it is possible to use this situation to determine the arrival time t_γ. Imagine that X-rays are absorbed in a scintillator microfiber or metal matrix array with position resolution 100μm, and the scintillator is viewed by a Bi-Directional CCD array with pixel pitch 50μm. The optical signal from the scintillator will then be seen simultaneously by pixels in at least two contiguous columns. As shown in Fig. 4, if columns are clocked continuously (i.e., if $t_{int} = 0$), with odd columns clocked upward and even columns clocked downward, then the signature of an event will be hits in two adjacent columns at $(i + t_\gamma / t_{row}, 2j + 1)$ and $(i - t_\gamma / t_{row}, 2j + 2)$. The actual row position is the average $\frac{1}{2}\left[(i + \frac{t_\gamma}{t_{row}}) + (i - \frac{t_\gamma}{t_{row}})\right]$, and the event arrival time is given by the difference $\frac{t_{row}}{2}\left[(i + \frac{t_\gamma}{t_{row}}) - (i - \frac{t_\gamma}{t_{row}})\right]$.

If there are n_{rows} rows, then the time to read out the entire array is $n_{rows}\, t_{row}$ (= 15 msec for the case of a 512 x 512 array clocking vertically every 30 μsec). The flux must be sufficiently low that the chances of seeing more than one event per two adjacent columns per full-frame readout time is small:

$$F < \frac{1}{2 n_{rows}^2 d^2 t_{row}} \tag{5}$$

where d is the pixel size. (For d = 50μm in the example above, the limiting flux is then 3 x 10^3 X-rays $cm^{-2}\ sec^{-1}$.)

For the 50 msec Loral readout, the train of 5 MHz horizontal clock pulses generates noise and draws power, as does the ADC (which must perform a pulse height conversion in 380 nsec). In the Bi-Directional concept, however, note that at the limiting flux, the average number of hits *per row* is $\frac{1}{2n_{row}} << 1$. In the case of a 100μm diameter spot viewed by 50μm pixels, an average of 4 pixels will be illuminated per hit, so the number of pixels per row will be $2/n_{row}$, which is still small. The complications imposed by the short ADC conversion time and fast horizontal clocking are therefore eased for the Bi-Directional CCD if a sparse readout is employed. By feeding the $n_{row}/2$ (e.g., 256 in the example above) outputs from the odd columns at the top through a multiplexor to a single ADC, and the $n_{row}/2$ outputs from the even (bottom) columns through a multiplexor to a second ADC, the horizontal clocking is eliminated and (allowing for a maximum of m pixels hit per row) the ADC conversion time becomes t_{row}/m (for m=10 in the example above, this is 3 μsec per ADC conversion).

The Bi-Directional CCD described above has been designed at Suni Imaging Microsystems, Inc. The array utilizes two-phase clocking, and is implemented as a collection of pixel columns with separate metal clock lines connecting to the polysilicon gates in each column. The direction of charge transfer is determined by the ordering of the polysilicon gates, which alternates from column to column. The independence of the clock lines guarantees that an electrical defect in a single column will not affect adjacent columns, and the closely-spaced metal lines between columns are driven identically, so metal-to-metal electrical shorts between these lines will have little effect.

Improving the time resolution while simultaneously slowing down the clocking can be expected to have a significant impact on both noise levels and charge transfer efficiency. The largest contribution to multi-phase CCD dark current is the thermal noise due to surface states at the $Si\text{-}SiO_2$ interface. If there is a large population of electrons in the valence band and unoccupied surface states available to accept the electrons, then electrons can jump from the valence band to form a dark current electron-hole pair. A technique to minimize this source of dark noise is the Multi-Pinned-Phase (MPP) approach, in which the vertical clocks are all left in the low state during the integration cycle. With a negative bias sufficiently low that the potential at the $Si\text{-}SiO_2$ interface drops below that of the substrate, holes from the channel stops will migrate into the interface, thereby filling the interface states and suppressing the valence electron transitions. However, when the clocks are switched from inverting to non-inverting in order to transfer the accumulated charge, some of the trapped holes will be ejected from the interface with sufficient velocity to release spurious electron-hole pairs by impact ionization. This impact ionization signal is minimized by slowing down the leading edge rise time of the clock pulse. In the case of a typical MPP CCD, the vertical registers are therefore operated inverted, but the faster horizontal registers are operated non-inverted in order to minimize the spurious impact ionization contribution. This is legitimate because the time required for the horizontal shifting is small, and so the build-up of dark noise is correspondingly small. In the Bi-Directional case, one has the advantages of both slow clocking and fast readout: Since the horizontal register is eliminated, the clock pulses are slow (t_{row} ~30 μsec) and so the leading edge rise times are correspondingly slow; and the full frame readout time is small ($N_{rows}t_{row}$ ~15 msec for a 512 x 512 array), so the dark noise build-up is small.

At low light levels, the pixel-to-pixel charge transfer is dominated by thermal diffusion with a time constant

$$\tau = \frac{4d^2}{\pi^2 D} , \tag{6}$$

where d is again the pixel size and D is the diffusion coefficient (D = 34.9 cm^2/sec for electrons in silicon at 300K, D = 12.4 cm^2/sec for holes). For the 15 μm pixels of the Loral 442 A, the electron diffusion time is τ = 26 nsec. For a 3-phase CCD, the charge transfer efficiency (for a single pixel) is

$$\mathrm{CTE} = (1 - e^{-t/\tau})^3 , \tag{7}$$

so that CTE can start to fall for sufficiently short time t. For example, CTE = 99.86% for t = 200 nsec, τ = 26 nsec. With this efficiency, only 24% of the charge will be transferred across 1024 pixels (half of a 30 mm Loral 442 A). In the case of a 512 x 512 (d = 50 μm pitch, t_{row} = 30 μsec) Bi-Directional CCD, however, τ = 290 nsec and CTE is no longer limited by thermal diffusion.

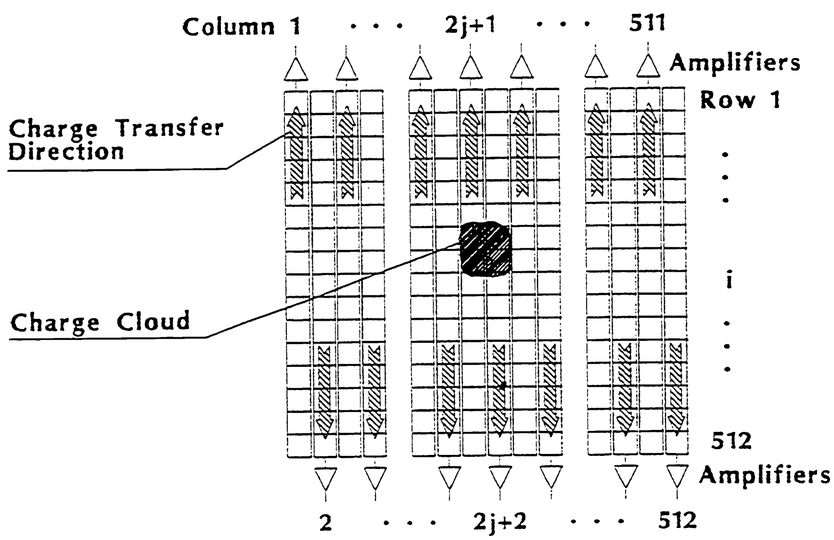

Figure 4. Bi-Directional CCD readout scheme.

4.2 CCD Readout

For the X-ray astronomy application at 50 keV, the CsI scintillator produces 20 optical photons/keV which are detected with 35% quantum efficiency by the CCD. If each photon produces 1 electron and the signal is split over 4 pixels, then the 50 keV threshold signal corresponds to approximately 90 e^-/pixel. If the total (readout plus thermal) noise is 10 e^-/pixel (rms), then the chance of spurious hits at the 9σ level simultaneously in 4 contiguous pixels in a 512 x 512 array is exceedingly small.

Thermal noise is reduced by shortening the frame readout time. The dominant noise contributor is then expected to be the on-chip amplifier. As the charge leaves the shift register, it is deposited on the gate of the output FET. The resulting voltage is $V = q/C$, where C is the associated output node capacitance. In order to increase the sensitivity, one decreases C - i.e., one makes the amplifier physically smaller. Before another charge packet is transferred out, however, the capacitor must be recharged to a fixed potential. This reference level has an uncertainty $(kTC)^{1/2} = 4.0 \times 10^8\ C^{1/2}\ e^-$ (rms) at room temperature, or $(kT/C)^{1/2}$ volts (rms) which increases with decreasing capacitance. The intrinsic 1/f noise of the output transistor also increases with decreasing size, so that there is a trade-off between sensitivity and output node read noise. In practice, the optimum geometric size for the amplifier turns out to be ~10-100 μm on a side. In the case of a $(25\ \text{mm})^2$ Bi-Directional Fast Timing CCD with 256 amplifiers across the top and 256 across the bottom, the required physical space (~100μm/amplifier) is available.

In the current Bi-Directional CCD designed at Suni, the primary on-chip amplifier is a source-follower type, for simple low-noise operation. In addition, the current design includes an experimental floating-gate amplifier with a bipolar junction transistor output stage. The floating-gate amplifier has been designed for low-noise, high-speed perfirmance. The choice of amplifiers is made via on-chip switches in series with the output pad.

Proper readout chain design is critical to low-noise CCD performance. For the BiDirectional CCD, with an independent amplifier chain for each column, the readout circuitry will be implemented in 1.2 μm CMOS directly on the CCD. A preliminary design has been developed by Lawrence Berkeley Lab and Suni Imaging Microsystems, Inc., based closely on the previous LBL designs for the SVX2 chip used at Fermilab[14,15] and the silicon detector on the ACE spacecraft cosmic ray heavy ion experiment. Two readouts will service each CCD, with a total footprint $<(2.6\ \text{cm})^2$. Each readout ASIC will have 256 input channels (i.e., 256 for the top, 256 for the bottom of the CCD). Each readout channel will have an independent preamplifier, amplifier, double correlated sampling noise suppression, sample and hold, and ADC with a 30 μs event clocking rate. The ADC uses a low-power Wilkinson converter with a Gray code counter sensitive to both rising and falling edges of a common clock measuring time-above-threshold of a decreasing ramp of all 256 channels. ADC resolution will be 9 bits, with a power dissipation ~2 mW/channel for the full readout chain.

Gain corrections will be necessary and will depend on frequent calibrations. An ^{241}Am X-ray source produces X-rays in coincidence with an alpha particle. If the source is imbedded in a small plastic scintillator viewed by a photomultiplier tube, than every X-ray is accompanied by a simultaneous α-particle pulse which gives a "calibration flag" from the PMT. If the calibration source is placed near the CCD but to the side out of the field of view, ~5% of the calibration flags may be accompanied by X-ray hits in the CCD, which can be recognized by the timing coincidence. (A similar method was used by Forrest et al.[16] for the continuous in-flight calibration of the Solar Maximum Mission Gamma Ray Spectrometer.)

A BiDirectional CCD designed at Suni has been fabricated using a 1.2 μm, 2-metal, 2-poly process. The first prototypes came off the fabrication line in June 1996, were DC-tested and packaged in July, and are currently undergoing full testing.

5. ACKNOWLEDGEMENTS

This work has been supported at LSU by NASA Astrophysics, NASA EPSCoR, and the Louisiana Board of Regents. At UNH, support has been provided by NASA Astrophysics. The CsI fabrication has been performed at Radiation Monitoring Devices, and we appreciatate the efforts and many helpful and valuable discussions with V. Nagarkar, S. Vasile, J. Gordon, and their colleagues at RMD.

6. REFERENCES

1. J. Paul et al., "Sigma – The Hard X-Ray and Soft Gamma-Ray Telescope on Board the Granat Space Observatory", Adv. Space Research 11, 289 (1991).
2. M.L. Cherry et al., "A New Balloon-Borne Detector for High Angular Resolution Hard X-Ray Astronomy", Proc. 24th Intl. Cosmic Ray Conf. (Rome) 2, 45 (1995).
3. M. McConnell et al., "A Balloon-Borne Coded Aperture Telescope for Arc-Minute Angular Resolution at Hard X-Ray Energies," to be published, SPIE Conf. Proc. 2806 (1996).
4. J.R. Macri et al., "Development of an Orthogonal-Strip CdZnTe Gamma Radiation Imaging Spectrometer", IEEE Trans. Nucl. Sci. 43, 1458 (1996).
5. J.R. Macri et al., "Progress in the Development of Large Area Sub-millimeter CdZnTe Strip Detectors", to be published in SPIE Conf. Proc. 2859 (1996).
6. V. Nagarkar et al., "Improved X-Ray Converters for CCD-Based Crystallography Detectors", SPIE Conf. Proc. 2519, 2 (1995).
7. S. A. Vasile et al., "Cost-Effective Segmented Scintillating Screens for Hard X-rays," to be published, SPIE Conf. Proc. 2859 (1996); V. Nagarkar, private communication.
8. W.E. Althouse et al., "A Balloon-Borne Imaging Gamma-Ray Telescope", Proc. 19th Intl. Cosmic Ray Conf. (LaJolla) 3, 299 (1985); S.M. Schindler et al., "GRIP-2: A Sensitive Balloon-Borne Gamma-Ray Telescope", submitted to Nucl. Instrum. and Meth. (1996).
9. P.P. Dunphy et al., "A Balloon-Borne Coded Aperture Telescope for Low-Energy Gamma-Ray Astronomy", Nucl. Instrum. Meth. A274, 362 (1989).
10. R. Sunyaev, "X-Ray Telescopes Art-P and Art-S for the GRANAT Project", Adv. in Space Res. 10, 233 (1990).
11. R.M. Nishikawa *et al.*, "Scanned-Projection Digital Mammography", Med. Phys. 14, 717 (1987).
12. M.J. Yaffe *et al.*, "Development of a Digital Mammography System", SPIE Proc. 914, 182 (1988).
13. J.M. Boone, "Color Mammography: Image Generation and Receiver Operating Characteristic Evaluation", Inv. Radiol. 26, 521 (1991).
14. S. Kleinfelder et al., "A Flexible 128 Channel Silicon Strip Detector Instrumentation Integrated Circuit with Sparse Data Readout," IEEE Trans. Nucl. Sci. 35, 171 (1988).
15. T. Zimmerman et al., "The SVX2 Readout Chip," IEEE Trans. Nucl. Sci. 42, 803 (1995).
16. D.J. Forrest et al., "The Gamma Ray Spectrometer for the Solar Maximum Mission," Solar Phys. 65, 15 (1980).